Optical and transport properties of new transition metal fluoride/graphite intercalation compounds (GICs)

K. Amine,* A. Tressaud, S. G. Mayorga,** J. Grannec, P. Hagenmuller
Laboratoire de Chimie du Solide du CNRS, Université de Bordeaux I, 33405 Talence Cedex (France)

L. Piraux, J. P. Issi
Unité de Physico-Chimie et de Physique des Matériaux, Université Catholique de Louvain, B-1348 Louvain-la-Neuve (Belgium)

and T. Nakajima
Department of Industrial Chemistry, Faculty of Engineering, Kyoto University, Kyoto 606 (Japan)

Abstract

The intercalation process of some d-transition metal fluorides in graphite has been investigated using anhydrous liquid HF C_xMF_y GICs have been obtained for M = Cr, Rh, Ir and Au. The charge transfer has been evaluated from optical reflectivity measurements. Comparison has been carried out between electrical conductivity obtained from optical data and from a contactless method. Results on the in-plane electrical resistivity and thermal conductivity are reported. All compounds exhibit a logarithmic resistivity divergence in the low-temperature range due to weak localization and carrier–carrier interaction effects for 2D metals

Introduction

A large number of fluoride intercalation compounds have been prepared over the past two decades [1]. Most of them are the result of gas–solid reactions involving graphite and a volatile fluoride species. For non-volatile fluorides, a solid–liquid intercalation reaction seems to be the most appropriate method. Recently, several new GICs have been obtained using anhydrous liquid HF (AHF) as solvent, including Cr- and Rh-based compounds [2–6]. In the present work, the intercalation reaction between graphite and AuF_3 or IrF_5 in AHF has also been investigated. McCarron [7] first attempted the intercalation of gold fluoride in graphite by exploiting the strongly oxidizing Au(V) dioxygenyl salt, $O_2^+AuF_6^-$, according to the following reaction:

$$C_x + O_2^+[AuF_6]^-(s) \longrightarrow C_xAuF_6(s) + O_2(g)$$

Current addresses: *Department of Industrial Chemistry, Kyoto University, Kyoto 606, Japan; **Air Products, Allentown, PA 18195-1501, USA

0022-1139/92/$5 00

In the absence of a suitable solvent for the dioxygenyl salt, only quite limited intercalation was observed. The direct intercalation of the binary fluorides, namely CrF_4, RhF_5, IrF_5 and AuF_3, in vacuum was attempted first at room temperature and then at higher temperatures (420–450 K). However, the AHF method was preferred since the intercalation speed seemed to be drastically enhanced.

This paper deals with the evaluation of the Fermi energy of some d-transition metal fluoride GICs from optical reflectivity data and with their electrical resistivity, thermopower and thermal conductivity properties. It should be mentioned that the XPS properties of these materials have been previously investigated [5, 8].

Experimental

The metal fluorides RhF_5, IrF_5 and AuF_3 were synthesized by fluorination of finely powdered metals. The oxidation was carried out at about $T \approx 620$ K following the reaction:

$$M + \frac{y}{2} F_2 \longrightarrow MF_y$$

Chromium tetrafluoride was prepared by direct fluorination of CrF_3. All these fluorides are moisture sensitive and must be handled only under extremely dry conditions.

Various types of host graphite were used: powdered natural graphite (SP1 grade from Union Carbide), highly oriented pyrolitic graphite (HOPG from Union Carbide), pitch-derived fibers (PDF from Osaka Gas Co.), and flaky natural graphite (NG) from Madagascar (0.2 to 1 mm in diameter). Prior to any reaction, adsorbed water was eliminated from the graphite by heating the sample at 770 K under vacuum.

The intercalation process was carried out in AHF which had been previously purified using perfluorinated inorganic species such as $M_2Ni^{IV}F_6$ or $M_3Cu^{III}F_6$ (M = alkali element). This method allowed us to eliminate traces of moisture and to saturate AHF with fluorine using procedures and equipment previously described [4].

The compositions of the GICs were determined from weight uptake, electron microprobe analysis using standard samples containing the same components in appropriate amounts, and from elemental analyses which were carried out at the CNRS Service Central d'Analyse and at Kyoto University. Powder diffraction techniques were used to determine the stage number, the repeat distance I_c along the c-axis, and the intercalate thickness. The X-ray diffraction spectra (XRD) were recorded on a Philips diffractometer using filtered Cu K_α radiation. Magnetic measurements were performed using a SQUID magnetometer (S. H. E. Corp.) in 4–300 K temperature range under an applied field of 0.5 T. Optical reflectivity experiments were carried from the UV to near-IR region using a SHIMAZU

UV-365 spectrometer. The incident beam was roughly parallel to the c-axis of the sample and PbS was used as a detector. The electrical resistivity measurements were achieved either with a contactless method or using a d.c. four-probe technique.

Results and discussion

Chemical and structural characterization

The obtained GICs have a reflective blue metallic appearance, in contrast with the dark grey color of the host graphite. Such a luster appears much more for Rh and Ir fluoride GICs than for AuF_3-based compounds. The materials exhibit different chemical behavior: C_xIrF_y is extremely sensitive to atmospheric moisture, whereas gold and rhodium fluoride GICs are air and moisture stable. Neither deterioration nor structural change is observed in the XRD spectra of samples left for 1 year under normal atmospheric conditions. Furthermore, the gold fluoride GIC can be washed in water or in HCl solution without any apparent structural change, and it is also stable with respect to dynamic gas evacuation. This property may suggest that no residual neutral HF molecules remain between the graphite layers.

The stage number of the obtained GICs is generally dependent on the nature of the starting graphite and on the metal fluoride-to-graphite molar ratio. A pure first stage is more easily obtained for powder SP1 graphite, whereas NG or HOPG generally leads to mixtures of high stages.

The reaction of chromium tetrafluoride on graphite gives stage-two compounds, whatever the starting graphite material. The repeat distance, $I_c = 11.45$ Å, is in good agreement with CrF_6 octahedra containing Cr(IV) [4]. For rhodium fluoride-based compounds, pure stage-one can be readily obtained with NG flakes, whereas HOPG leads to stage-two compounds. The corresponding repeat distances (I_c) are 7.87 Å and 11.25 Å, *i.e.* values which are in good agreement with intercalated species of approximately 4.5 Å in thickness. For each pattern, the XRD peaks are broad due to a somewhat disordered distribution of the intercalates. For C_xAuF_y, pure first- or second-stage compounds can be readily obtained in the case of SP1 or NG, whereas HOPG yields either a second-stage compound or mixtures in which the second stage is predominant. However for C_xIrF_y, either pure first-stage or second-stage compounds can be obtained regardless of the starting pristine graphite. The interlayer carbon spacing I_c along the c-axis leads to an intercalate thickness of about 4.5 to 4.8 Å.

The fitting of the intensities of the $(00l)$ powder diffraction lines of C_xCrF_y leads to a theoretical $C_{18}CrF_{4.5}$ formulation, which is in good agreement with the observed composition, *i.e.* $C_xCrF_{4.5}$ with $17 \leqslant x \leqslant 21$. The elemental analysis of HOPG-based rhodium fluoride GICs (stage-two)

yields the formula $C_{28}RhF_{3.3}(HF_2)_{1.3}$ which confirms the co-intercalation of both groups. Gravimetric analyses of a number of samples of iridium fluoride GICs (stage-two, HOPG-based) showed an average weight uptake of 170%. The corresponding composition $C_{14}IrF_5$ is in reasonable agreement with that obtained from elemental analysis: $C_{14\pm1}Ir_{1\pm0.1}F_{4.9\pm0.2}$. For the HOPG-based gold fluoride compound, an approximate weight uptake of either 300% or 150% is observed, depending on the stage of the final compound (stage-one or two respectively): the estimated compositions are C_7AuF_3 and $C_{12}AuF_3$, assuming neither incorporation of HF nor change of the gold oxidation state. Electron microprobe analyses performed on a series of stage-one NG-based compounds gave the average composition: $C_{6\pm2}Au_{1\pm0.1}F_{4.2\pm0.2}$. The elemental analysis of HOPG-based stage-two material led to $C_{12\pm2}Au_{1\pm0.1}F_{3.2\pm0.2}$.

More detailed information on the structural characteristics of these GICs can be found in ref. 8. In addition, XPS, magnetic and EXAFS investigations have shown that in these compounds Rh and Au have a diamagnetic trivalent oxidation state (III) configuration, whereas a paramagnetic tetravalent state was obtained for Cr- and Ir-based materials [4, 8].

Optical reflectivity

In the transition metal fluoride GICs studied, a metallic reflectivity is observed in the low-frequency region of the spectrum limited by the plasma

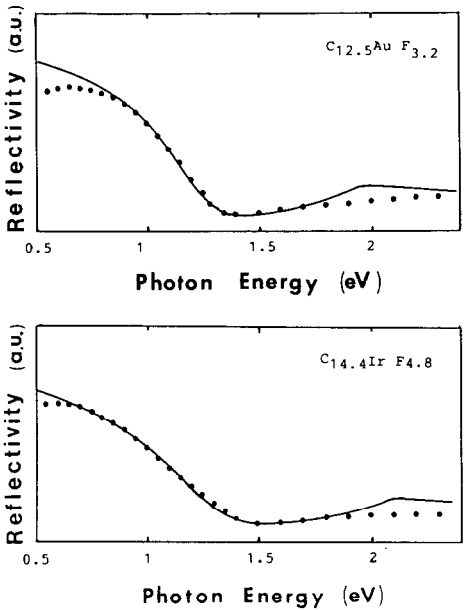

Fig. 1. Reflectivity spectra of $C_{12.5}AuF_{3.2}$ and $C_{14.4}IrF_{4.8}$ at room temperature.

edge and followed by a well-pronounced minimum. The reflectivity spectra of C_xIrF_y and C_xAuF_y compounds at room temperature are given as examples in Fig. 1. The dots correspond to the experimental points and the solid line to a theoretical fitting using the Blinowski–Rigaux model [9].

Using this model, the position of the Fermi level (E_F) can be related to the charge transfer coefficient f which is defined for the stage-two C_xMF_y compound as the number of holes per intercalated species:

$$E_F = \gamma_o \sqrt{\pi f \sqrt{3}/x}$$

where $\gamma_o = 2.9$ eV is the overlapping integral between the electron wave functions of the nearest-neighbor carbon atoms in the same plane. Theoretical fitting of experimental spectra has been performed by adjusting E_F and the damping factor τ. In Table 1 are reported E_F and τ values for which the best fitting to the experimental spectra has been achieved. Charge-transfer coefficient, electrical conductivity derived from optical reflectance (σ_{opt}), and electrical conductivity obtained by the contactless method (σ_{clm}) are also compared. The value σ_{opt} is determined using a Drude equation approximation ($\sigma = ne^2\tau$):

$$\sigma_{opt} = \omega_p^2 \tau / 4\pi$$

with

$$\omega_p = E_F \times 4e^2/\hbar^2 I_c$$

It can be noted from Table 1 that the discrepancy between σ_{opt} and σ_{clm} is relatively large for Cr(IV)- and Ir(IV)-based GICs, whereas relatively close values are obtained for diamagnetic $C_xAu^{III}F_y$. The estimation of electrical conductivity by the contactless technique is based on eddy currents induced by a magnetic field and could therefore be perturbed by the presence of paramagnetic material.

Transport properties

A significant feature of low-stage metal fluoride GICs is their relatively low electrical conductivity compared to other typical GICs. For most low-stage GICs, intercalation always gives rise to a conductivity enhancement with respect to the pristine material. This is not the case using fluorine [10, 11] or transition metal fluorides [12] as the intercalate species. Some conductivity values of second-stage C_xMF_y compounds are reported in Table 1. While for most low-stage acceptor GICs the conductivity increases by about one order of magnitude with respect to the pristine material, the conductivities of second-stage C_xMF_y compounds are similar or even smaller than that of pure HOPG ($\sigma(300\text{ K}) \approx 2.5 \times 10^4$ S cm^{-1}).

In contrast, the Fermi energies of these C_xMF_y compounds are of the same order of magnitude as those usually reported for second-stage acceptor GICs [9], suggesting that strong defect scattering rather than low charge density is responsible for the low conductivity. As expected,

TABLE 1

Parameters obtained from the fitting of the experimental data using the Blinowski–Rigaux model

Compounds[a] (HOPG-based)	Stage	I_c (Å)	E_F (eV)	τ (s) $\times 10^{-14}$	f_C	f_m	σ_{opt} (S cm^{-1}) $\times 10^4$	σ_{clm} (S cm^{-1}) $\times 10^4$	Ref.
$C_{21}CrF_{4.5}$	2	11.45	0.94	2.8	0.024	0.50	5.2 [6]	0.7	[b]
$C_{28}RhF_{3.3}(HF_2)_{1.3}$	2	11.25	0.89	1.2	0.021	0.59	2.2	—	6
$C_{14.4}IrF_{4.8}$	2	11.47	1.03	0.73	0.023	0.33	1.5	0.65	[b]
$C_{12.5}AuF_{3.2}$	2	11.57	0.97	1.06	0.020	0.25	2.0	1.94	[b]

[a]The compositions have been deduced from elemental analyses.
[b]This work.

such a strong defect scattering enhances the quantum phenomena of weak localization and carrier–carrier interaction usually observed in 2D disordered metals. These phenomena are responsible for the apparently non-metallic behavior in the temperature dependence of the resistivity, as illustrated in Fig. 2. Starting from the lowest temperatures, a logarithmic decrease of resistivity with increasing temperature is observed. The magnitude of the effect seems to be, in fact, very sensitive to the nature of graphite host material. For the intercalated HOPG samples (Fig. 2a), the logarithmic behavior of the resistivity is restricted to the low-temperature range with correspondingly small resistivity *vs.* $\ln T$ slopes (0.1–1% change in resistivity over a temperature decade). Around 10–20 K, the resistivity shows a minimum, then increasing resistivity occurs with rising temperature. In contrast, for some intercalated pitch-derived fibers (Fig. 2b), we found that these quantum corrections to the resistivity completely determine the temperature variation of the resistivity up to room temperature. For such compounds, the rate of the logarithmic variation of resistivity is also much larger than that observed for intercalated HOPG samples, *i.e.* 10–20%. At $T = 4.2$ K, the resistivity for the PDF–CrF_y and the PDF RhF_y samples are $26 \times 10^{-3}\ \Omega$ cm and $1.4 \times 10^{-3}\ \Omega$ cm, respectively.

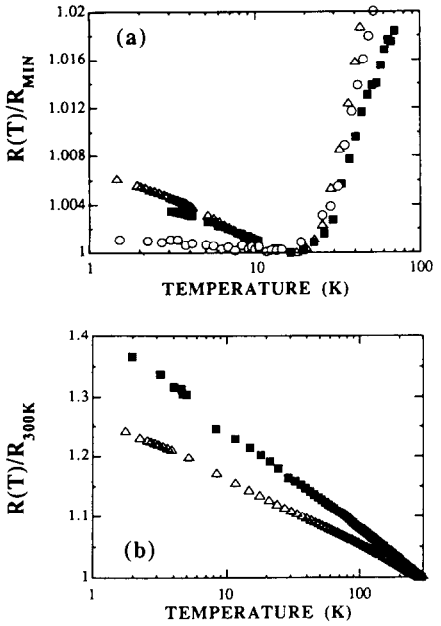

Fig. 2. Resistivity *vs.* temperature on a logarithm scale for metal fluoride GICs: (a) HOPG–AuF_y (○), HOPG–CrF_y (■) and HOPG–RhF_y (△); (b) PDF–CrF_y (■) and PDF–RhF_y (△). The data in (a) and in (b) are normalized to the minimum value of resistance and to the room temperature value, respectively.

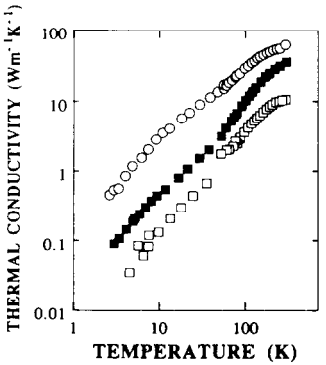

Fig. 3. Temperature variation of the thermal conductivity of HOPG–AuF_y (○), HOPG CrF_y (■) and PDF-CrF_y (□) compounds.

In the same way that the magnitude of the logarithmic divergence of the resistivity depends on the structural disorder, the thermal conductivity also exhibits disorder dependence. Such sensitivity to the degree of disorder concerns both lattice and electronic components in the thermal conductivity. Figure 3 shows the temperature dependence of the in-plane thermal conductivity of HOPG–AuF_y, HOPG–CrF_y and PDF–CrF_y compounds in the temperature range $3 \leqslant T \leqslant 300$ K. As expected, the lower the thermal conductivity, the lower the electrical conductivity (see data of Table 1 and the resistivity values for intercalated PDF mentioned above in the text) and the larger the slope of the ln T dependence of resistivity. As emphasized in a recent paper [12], we may also note that, contrary to most acceptor GICs where an electronic contribution to heat transport occurs especially at low temperature [13], the thermal conductivity of the PDF–CrF_y sample seems to result entirely from phonons over the whole temperature range investigated.

Acknowledgements

This study has been carried out in the scope of a CNRS–JSPS Cooperation Program. The authors are indebted to Osaka Gas Co. Ltd. and Dr H. Fujimoto for having provided them with pitch-derived fibers. ATOCHEM is acknowledged for awarding a Chateaubriand fellowship to one of us (S.G.M.).

References

1 N. Watanabe, H. Touhara, T. Nakajima, N. Bartlett, T. Mallouk and H. Selig, in P. Hagenmuller (ed.), *Inorganic Solid Fluorides*, Academic Press, New York, 1985, chapt. 8, p. 331.

2 T. Mallouk and N. Bartlett, *J. Chem. Soc. Chem. Commun.*, (1983) 103.
3 H. Touhara, K. Kadono, H. Imoto, N. Watanabe, A. Tressaud and J. Grannec, *Synth. Met.*, *18* (1987) 549.
4 K. Amine, A. Tressaud, H. Imoto, J. Grannec, J. M. Dance and C. Hauw, *J. Solid State Chem.*, *96* (1992) 287.
5 K. Amine, A. Tressaud, H. Imoto, E. Fargin, P. Hagenmuller and H. Touhara, *Mat. Res. Bull.*, *26* (1991) 337.
6 K. Amine, A. Tressaud, P. Hagenmuller, H. Imoto, H. Touhara and T. Nakajima, *Mat. Res. Bull.*, *25* (1990) 1219.
7 E. McCarron, *Ph.D. Thesis*, University of California, Berkeley, 1978.
8 A. Tressaud, K. Amine, S. G. Mayorga, E. Fargin, J. Grannec, P. Hagenmuller and T. Nakajima, *Eur. J. Solid State Inorg. Chem.*, (1992), in press.
9 See, for example, C. Rigaux, in *Proceedings 10th Course Erice Summer School, International School of Materials Science and Technology, Erice, Sicily, Nato ASI Series; Series B, Physics*, Plenum Press, New York, 1986, p. 235.
10 D. Vaknin, I. Palchan, D. Davidov, H. Selig and D. Moses, *Synth. Met.*, *16* (1986) 349.
11 L. Piraux, V. Bayot, J. P. Issi, M. S. Dresselhaus, M. Endo and T. Nakajima, *Phys. Rev. B*, *41* (1990) 496.
12 L. Piraux, K. Amine, V. Bayot, J. P. Issi, A. Tressaud and H. Fujimoto, *Solid State Commun.*, *82* (1992) 371.
13 J. P. Issi, in S. Solin and H. Zabel (eds.), *Graphite Intercalation Compounds*, Vol. II. *Transport and Electronic Properties. Springer Series in Materials Science*, Springer Verlag, Berlin, 1992, in press.